Supporting Information for: Membrane anchoring of Hck kinase via the intrinsically disordered SH4-U and lengthscale associated with subcellular localization

Matthew P. Pond[a], Rebecca Eells[b], Bradley W. Treece[b], Frank Heinrich[b,d], Mathias Lösche[b,c,d], and Benoît Roux[a,*]

[a]Department of Biochemistry and Molecular Biology, Gordon Center for Integrative Science, University of Chicago, Chicago, IL 60637
[b]Department of Physics, Carnegie Mellon University, Pittsburgh, PA 15213
[c]Department of Biomedical Engineering, Carnegie Mellon University, Pittsburgh, PA 15213
[d]Center for Neutron Research, NIST, Gaithersburg, MD 20899
[*]Correspondance: roux@uchicago.edu

November 22, 2019

Protein production and purification

As described previously,[1] competent BL21(DE3) E. coli were transformed with a modified pET28a vector containing the coding sequence for residues 1-79 of human Hck and an N-terminal TEV-cleavable His6 tag, and used to inoculate a 60 mL starter culture in either Terrific Broth or M9 minimal medium. Following overnight growth at 37 °C the culture was scaled up to 1 L and grown to an OD_{600} of 0.8 after which the medium was cooled down to 18 °C and protein production was induced with 1mM IPTG. Cells were harvested after 20 hrs of additional growth and frozen at -80 °C for up to one month. To purify Hck_{SH4-U}, cells were homogenized, centrifuged, and purified using Ni-NTA chromatography. The His-tag was cleaved with TEV and removal of imidazole was accomplished by dialysis. The resulting sample was then re-passed over Ni-NTA to remove TEV and any remaining His-tagged Hck_{SH4-U}. Samples were exchanged into the desired buffer (50mM PIPES 5mM TCEP pH 6.7 for NMR, 50 mM Tris 5mM TCEP pH 8.0 for NR) and purified using a Superdex 200 column on an ÄKTA FPLC.

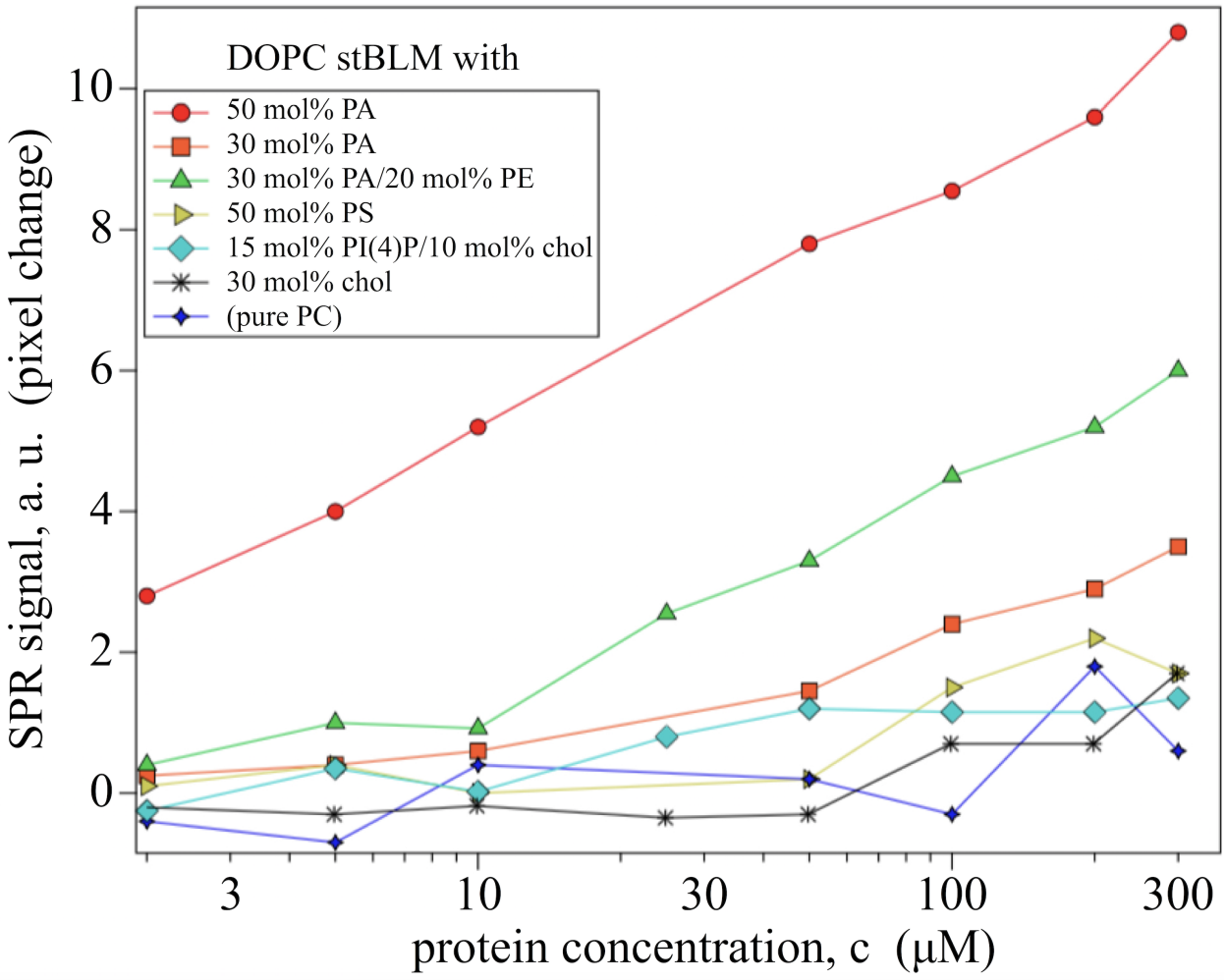

Figure S1: SPR response for Hck_{SH4-U} binding to bilayers of various lipid compositions by SPR. Symbols represent data points that were corrected for increases of the solutions refractive index due to dissolved protein (the lines connecting the data points have been added as a visual guide).

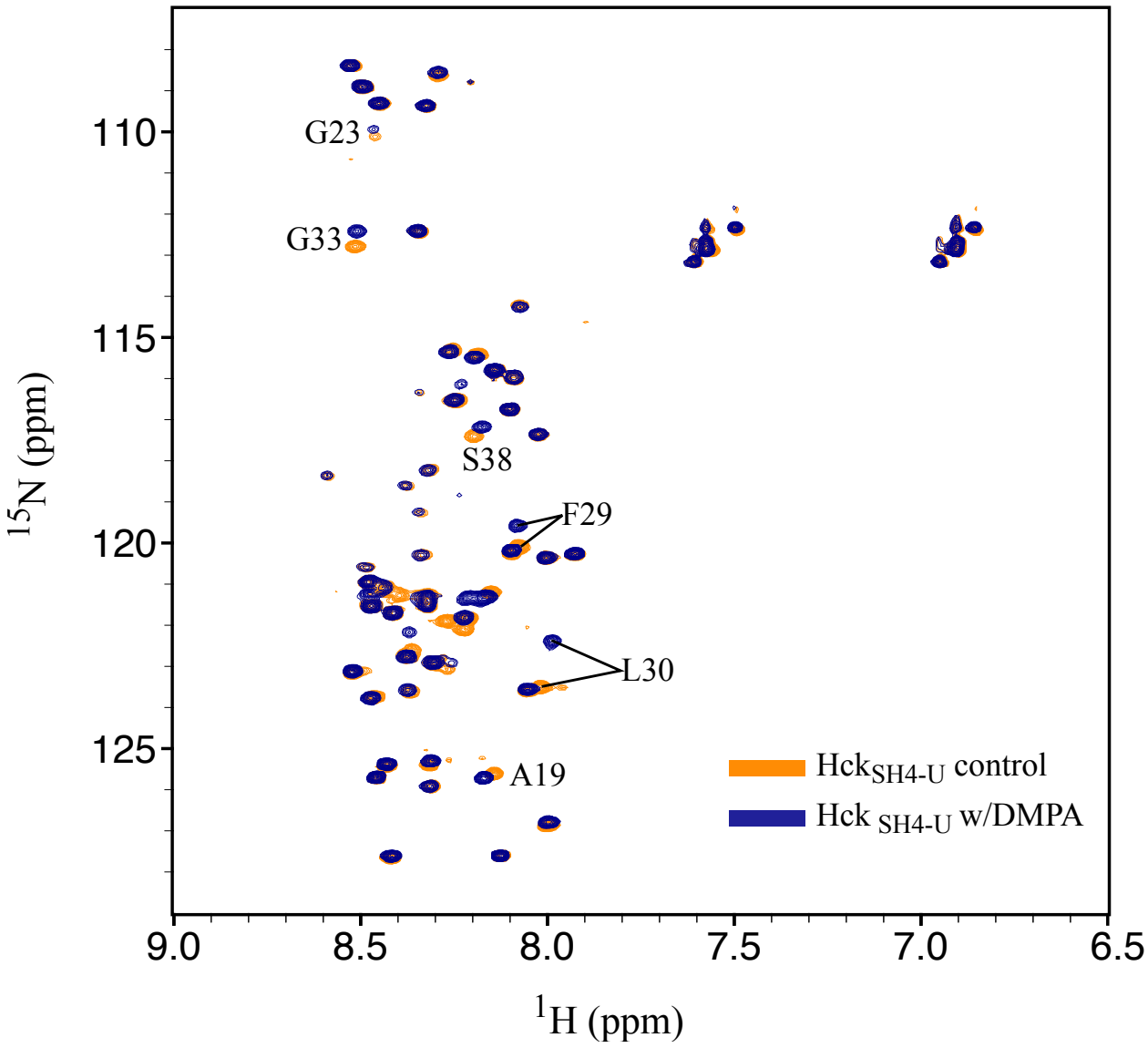

Figure S2: HSQC spectra of Hck$_{SH4-U}$ in the presence (blue) and absence (orange) of 80:20 DMPC:DMPA bicelles in 50mM PIPES 5mM TCEP pH 6.7 25°C. The perturbations are localized to the region spanning Arg18 to Thr40.

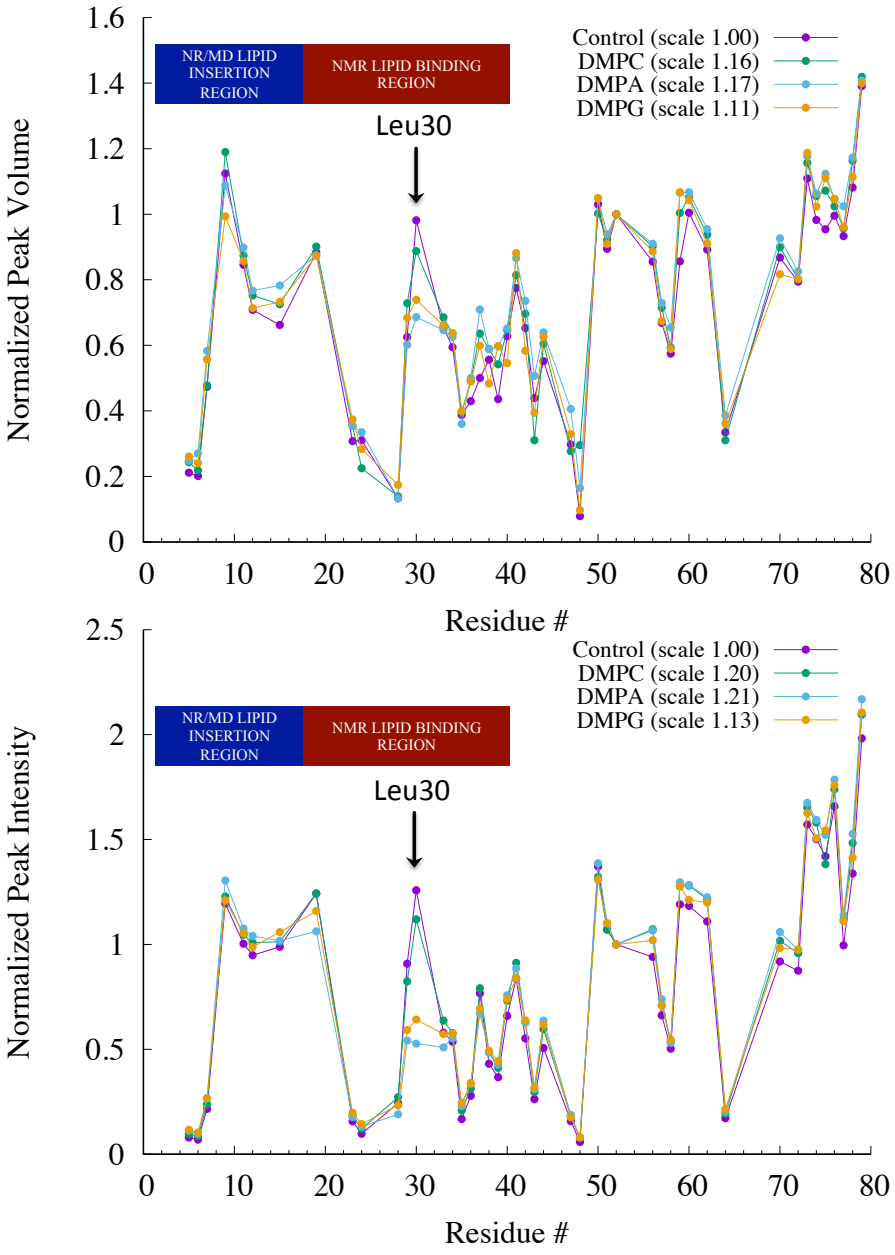

Figure S3: NMR ^{1}H-^{15}N HSQC crosspeak volumes (top) and crosspeak intensities (bottom) for $\mathrm{Hck}_{\mathrm{SH4-U}}$ in the presence and absence of lipid bicelles. The data are normalized to the value of Val52 in each spectrum and scaled with respect to each other for comparison. Association of $\mathrm{Hck}_{\mathrm{SH4-U}}$ with bicelles does not appear to induce a loss of signal or substantial line broadening for the N-terminal region of the protein identified from the NR restrained MD simulations as inserted into the membrane, arguing against the presence of this type of membrane association in the NMR sample. The line broadening and loss of signal intensity in the vicinity of Leu30 is limited to only the nearest neighbors and not other amino acids identified as interacting with the membrane and is interpreted as $\mathrm{Hck}_{\mathrm{SH4-U}}$ being in fast exchange between bound and unbound states with local conformational heterogeneity on the μs-ms timescale of Leu30 in the lipid bound state.

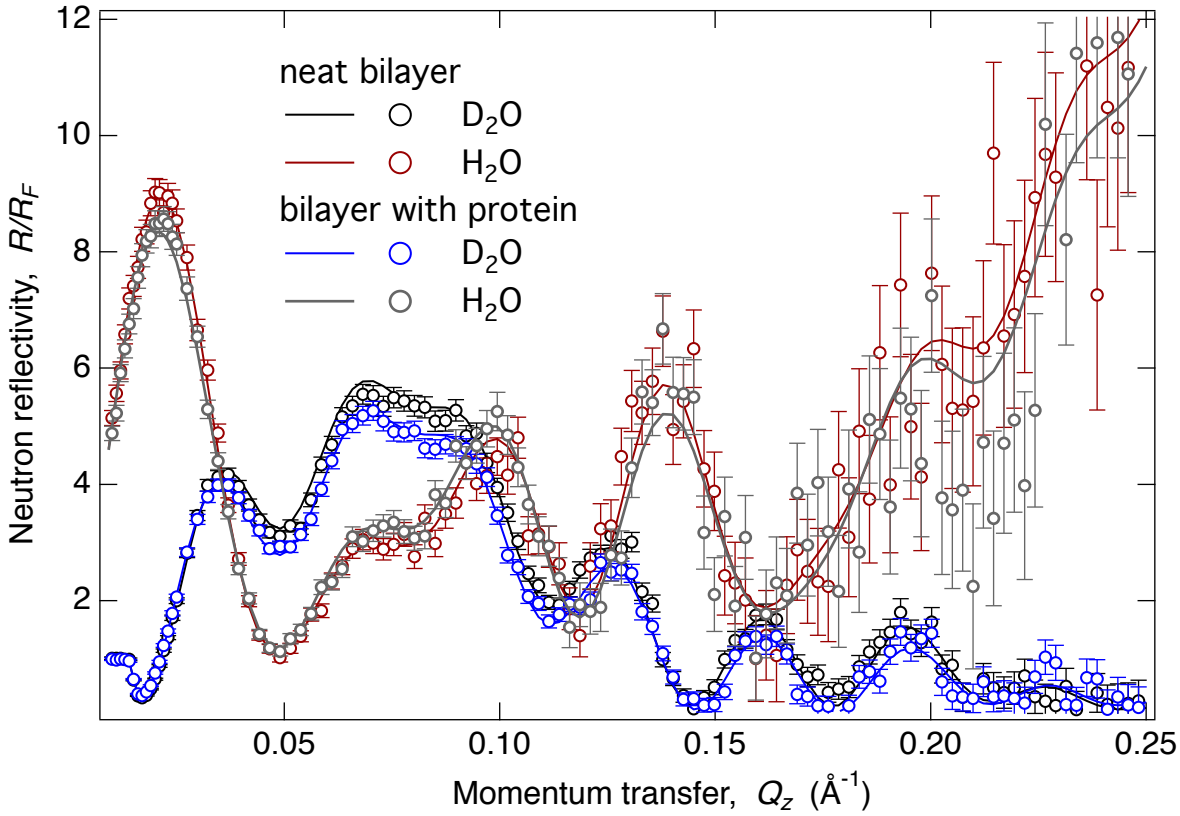

Figure S4: Exemplary NR results for $\mathrm{Hck_{SH4-U}}$ adsorbed from solution (for 50 μM $\mathrm{Hck_{SH4-U}}$) to an stBLM (DOPC/DOPA 50:50). The data have been scaled by the Fresnel reflectivity RF the reflectivity of an ideal, flat interface to emphasize the interference patterns that result from the surface-supported naked or the protein-decorated bilayer. Solid lines represent the reflectivities in which all four data sets have been fitted to one single model in which invariant parameters (such as the substrate structure) have been shared. This procedure constrains the model strongly and leads to the result shown in Fig. 4 of the main paper.

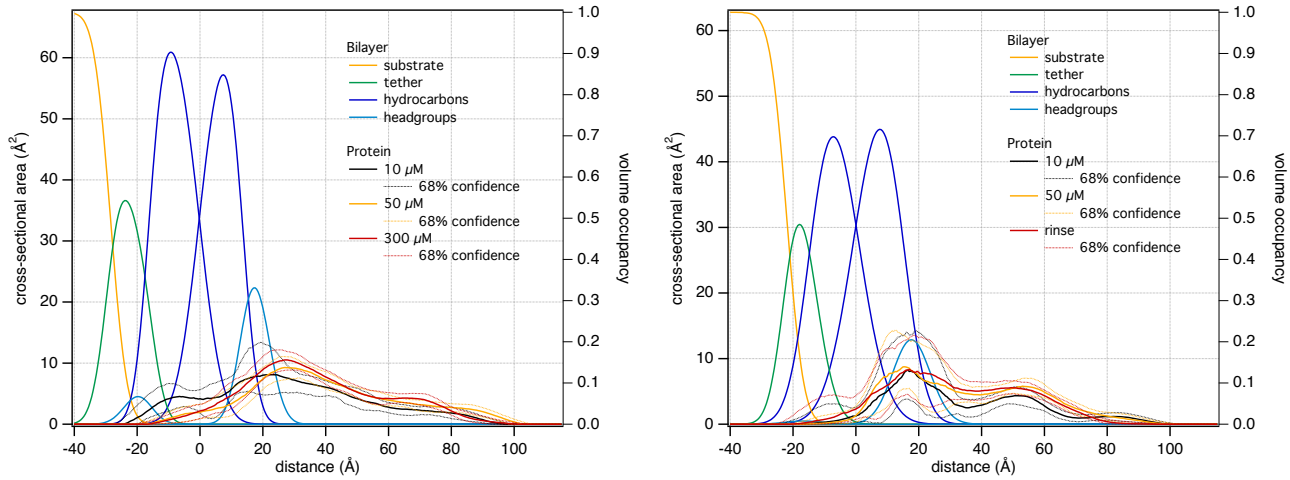

Figure S5: NR profiles for $\mathrm{Hck_{SH4-U}}$ SH4-U on PA-containing stBLMs. (Left) Three concentrations, 10 μM (black), 50 μM (orange), and 300 μM (red), on a 50:50 DOPA:DOPC stBLM measured after a rinse step. (Right) Two incubations, 10 μM (black) and 50 μM (orange), and a post-rinse measurement (red) on a 30:70 DOPA:DOPC stBLM. For all conditions there is a significant amount of protein at the interface and it is partially inserted. However, instrumental difficulties introduced a large uncertainty on the 30% PA measurement.

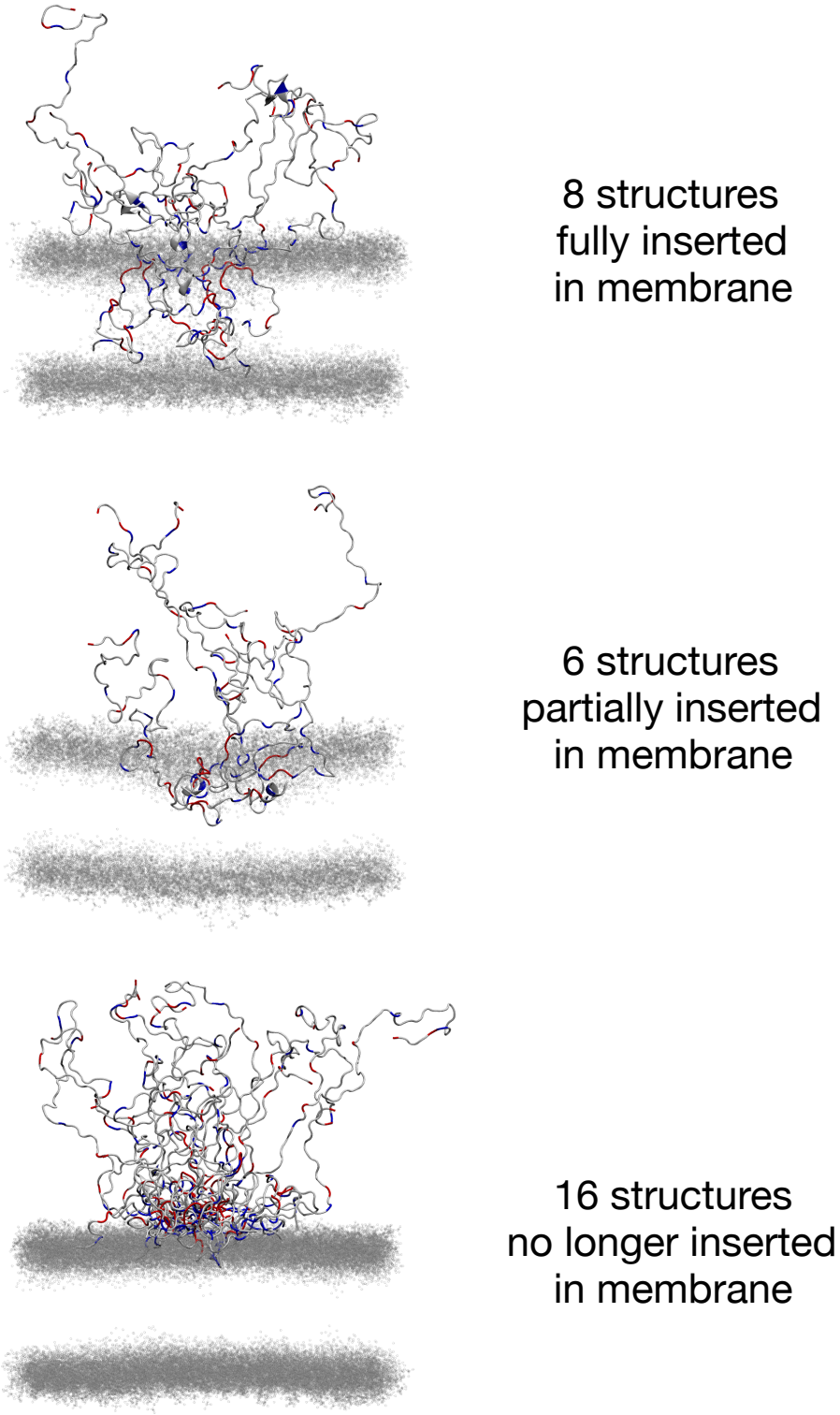

Figure S6: Structures from the ensemble produced from the re-MD procedure clustered by degree of membrane insertion and colored by charge. Acidic residues are colored in red and Basic residues are colored in blue . The polar headgroup atoms are show to indicate the membrane surface.

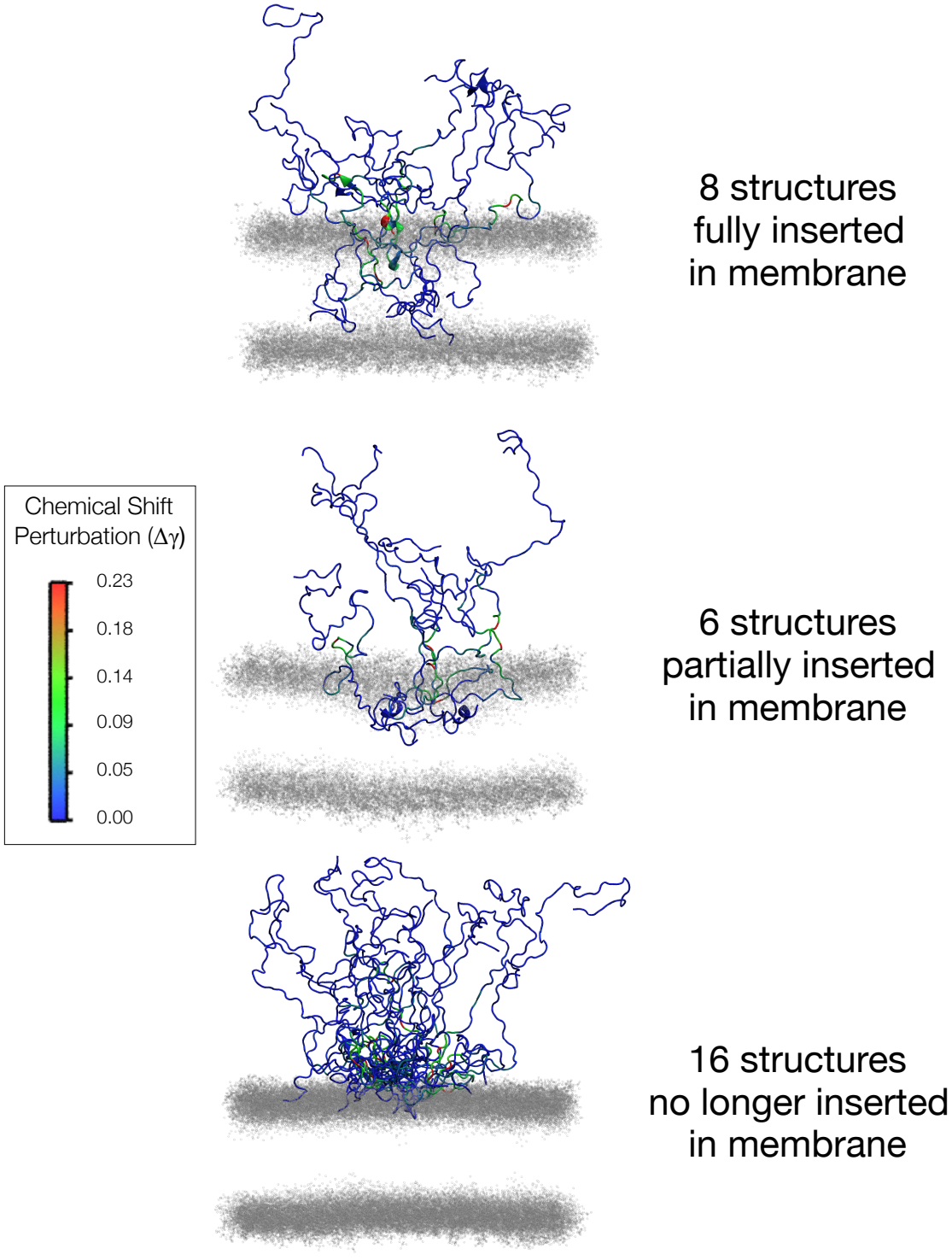

Figure S7: Structures from the ensemble produced from the re-MD procedure clustered by degree of membrane insertion and colored by the NMR chemical shift perturbations measured in the presence of PA containing bicelles. . The polar headgroup atoms are show to indicate the membrane surface.

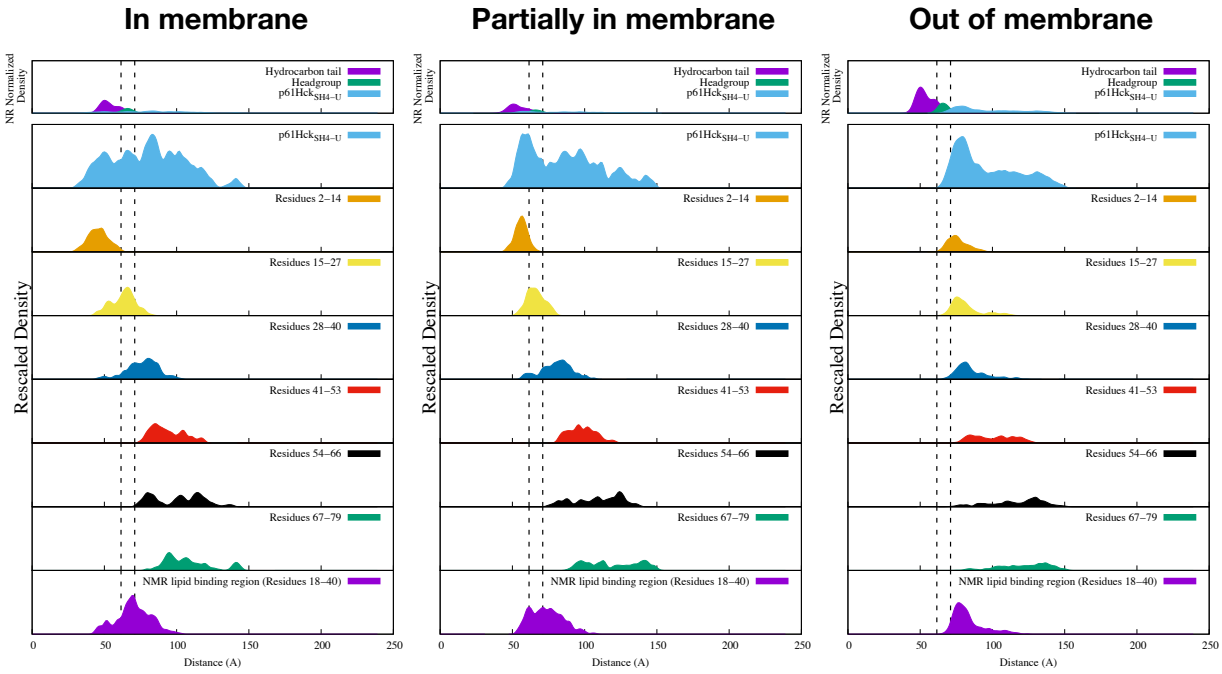

Figure S8: Segmental density profiles from the clusters shown in Figs. S6 and S7. The top panel in each column shows the relative contributions from each cluster (from left to right: 8 structures fully inserted into in the membrane, 6 structures partially buried in the membrane, and 16 structures that have no density beyond the lipid headgroups) to the profile seen in Fig. 3 in the main text, the remaining panels have been normalized for comparison across clusters.

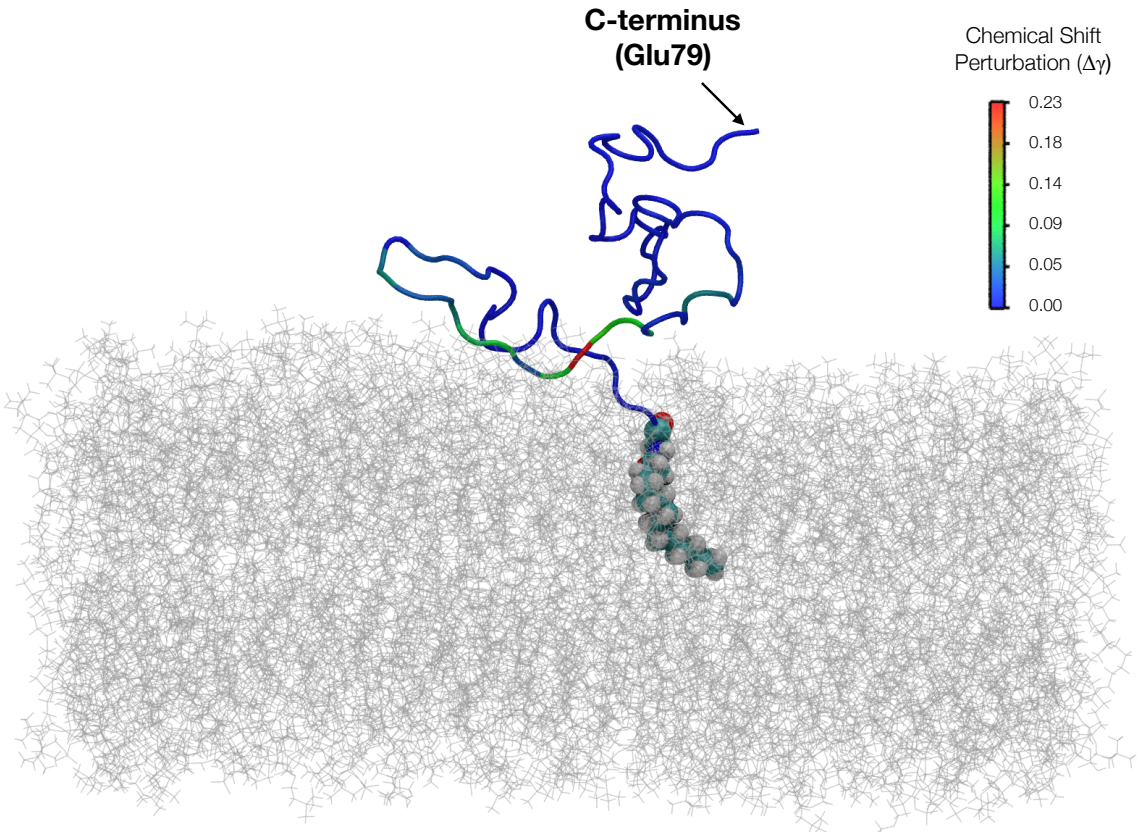

Figure S9: Structural model of myristoylated $\mathrm{Hck}_{\mathrm{SH4-U}}$ produced by lipidating a member of the ensemble generated from re-MD with the N-terminus near the membrane-solvent interface. The model was equilibrated by running 1 ns of unrestrained molecular dynamics in explicit solvent.

References

[1] M. P. Pond, L. Blachowicz, B. Roux, ^{1}H, ^{15}N, ^{13}C, resonance assignments of the intrinsically disordered SH4 and Unique domains of Hck, Biomol NMR Assign 1 (2019) 71–74.